Entomologia Generalis
Published online August 2024

Open Access
Early Access Article

Unveiling a cost of mutualism involving insect-endosymbiont-microbe interactions

Mengqi Xiao[1,], Feiyu Duan[1,**], Ary A. Hoffmann[2], Jiayao Hu[1], Fan Yang[1], Huimin Zhong[1], Jiqin Jia[1], Yimin Zhang[1], Xiaoying Wei[1], Jianqing Zhu[3], Weidong Yu[4], Weibin Jiang[1,5]**

[1] Laboratory of Environmental Entomology, College of Life Sciences, Shanghai Normal University, 100 Guiling Rd., Shanghai 200234, China
[2] School of BioSciences, Bio21 Institute, The University of Melbourne, Parkville, Victoria 3052, Australia
[3] Shanghai Zoological Park, 2381 Hongqiao Rd., Shanghai 200335, China
[4] College of Continuing Education, Shanghai Normal University, 100 Guiling Rd., Shanghai 200234, China
[5] Yangtze River Delta Urban Wetland Ecosystem National Field Scientific Observation and Research Station, Shanghai 201722, China
* Corresponding author: jiangwb@shnu.edu.cn
** These authors contributed equally to this work.

With 3 figures and 1 table

Abstract: Microbe-microbe interactions – of central importance in biological systems – can be antagonistic or synergistic, acting to benefit or detriment of a host. Pederin-producing endosymbionts (PPE) are considered protective mutualists in their *Paederus fuscipes* (rove beetle) hosts but little is known about whether PPE affect other aspects of host fitness as well as host microbial diversity. We find strong deleterious costs of PPE infections on hosts related to an extended development time, smaller and shorter lifespan of females, as well as a lower hatching rates of progeny. 16S rRNA data reveal that PPE affect the microbiome of *P. fuscipes* depending on gender and organ, resulting in a decrease in the number of the potentially beneficial symbiotic bacteria *Apibacter* and the reproductive manipulator *Wolbachia* and an increase in the conditional pathogenic bacterium *Bartonella*. Predicted microbe functions related to metabolism, longevity, immunity and resistibility are enriched in uninfected females, potentially contributing to fitness costs of PPE infections. We further sequence and annotate the first complete genome of PPE and compare the pederin biosynthetic gene cluster (*ped*) with the pederin family biosynthetic gene cluster from other bacterial-eukaryote symbioses. This study highlights the fitness costs of PPE infections to *P. fuscipes*, even though the defensive pederin compound produced by PPE helps protect the host. The ecology and evolution of this mutualism is shaped by costs, not just the benefits they confer. Changes in the microbial community within infected rove beetles may mediate the negative impacts of PPE on fitness.

Keywords: Pederin; endosymbionts; *Paederus fuscipes*; comparative genomics; gut microbiome

1 Introduction

The field of microbial ecology provides insights into the ecological and evolutionary dynamics of microbial communities underpinning every ecosystem on Earth. A leading question in this field (Antwis et al. 2017) concerns the primary mechanisms within a host that mediate microbe-microbe and host-microbe interactions. Associations with bacteria within insects are thought to have contributed to host life history traits such as behaviour, fitness, reproduction, detoxification, immunity and nutrient compensation (McCutcheon et al. 2019; Willing et al. 2011). In return, insects are thought to have evolved ways of facilitating the colonization and proliferation of some bacteria (Douglas 1998). Despite the significance of insect-microbe interactions, microbe-microbe interactions within insects represent an important, complex, dynamic network that warrants deeper investigation (Geller & Levy 2023). These have not been studied much because the complexity of the insect microbiome has hindered the direct evidence for the association between the target microbial species or strains.

Our recent study (Fang et al. 2023) discovered a facultative mutualism involving an insect-endosymbiont association, where endosymbionts in the rove beetle *Paederus*

DOI: 10.1127/entomologia/2024/2463
E. Schweizerbart'sche Verlagsbuchhandlung, 70176 Stuttgart, Germany, www.schweizerbart.de

fuscipes produce the toxic substance pederin (Kellner 2001), which protects the beetles from insect and arachnid predators. The beetle host, in return, provides a favorable environment for the colonization of Gram-negative pederin-producing endosymbionts (PPE) in female reproductive tissues (Fang et al. 2023). However, Teoh & Singham (2022) predicted the function of the microbiota of *P. fuscipes* and found some functions related to metabolism enriched in PPE uninfected females which are fitness advantage possibilities in sustaining the population in the absence of predation. A substantial body of work has demonstrated that defensive toxins are often costly for prey in the absence of predation risk (Zvereva & Kozlov 2016). In other host-endosymbiont systems, *Cardinium* and the combined *Cardinium* + *Wolbachia* infections were connected to negative fitness effects on their host, the planthopper *Sogatella furcifera*, which reduced microbiome diversity and affected host metabolism and fecundity (Li et al. 2022). The *P. fuscipes*-PPE association might therefore be complicated and we address this with the following questions. (i) Is there a fitness cost for PPE infections and what are the specific symbiont-mediated phenotypes of *P. fuscipes*? (ii) Could the fitness costs of PPE involve interactions with the host microbiome?

PPE is closely related to the well-known human pathogen *Pseudomonas aeruginosa*. Kellner (2001) found a putative pederin biosynthetic gene cluster (*ped*) from the genome of *P. fuscipes* and traced it to this bacterial symbiont. Based on fluorescence in situ hybridization (FISH), PPE are noted in female reproductive tissues of the rove beetle and concentrated in ovaries, but rare in male reproductive tissues (Fang et al. 2023; Kador et al. 2011). However, pederin is found widespread in different parts of the insect's body. Bhandari et al. (2015) used mass spectrometry imaging to locate pederin mainly in the defensive gland with reservoirs located at the posterior border of the 4th sternite, malpighian tubules, midgut, rectum, and ovaries of the female rove beetle. Some of the pederin in the glandular reservoir of the defensive gland protecting against predators is probably carried inside cells by norspermine because the vector for norspermine was detected in a high concentration close to pederin (Stromgaard et al. 2001). Other pederin is absorbed by malpighian tubules from the hemolymph and discharged to the transition of the midgut and rectum, where it may influence the composition and relative abundance of gut bacteria. A summary of the current understanding of these interactions in the rove beetle is outlined in Fig. 1.

We postulate here that PPE through the production of pederin may have a direct effect on the diversity of the microbiome in reproductive organs and an indirect effect on the diversity of the gut microbiome, and that this may indirectly alter the fitness of rove beetles. We firstly examine total development time, adult life span, body length and weight of the rove beetles with or lacking PPE. We then use 16S ribosomal RNA (rRNA) gene amplicon sequencing to examine the diversity and composition of the microbiome in reproductive organ and gut of *P. fuscipes* with a different gender and PPE infection status. Finally, we sequenced the genome of PPE and explored the genomic features associated with pederin production.

2 Materials and methods

2.1 Fitness effects of PPE

In order to assess PPE effects on fitness of the rove beetles, two *P. fuscipes* lines with a different infection status were established: a PPE-infected line (abbreviated as PIL) and a PPE-uninfected line (abbreviated as PUL). The two lines were established from 12 pairs of adult beetles collected in the same farmland of Nanyang, Henan province, China (N 34°39′; E 112°23′) in May, 2022. We divided the eggs laid by each pair into two groups. Eggs of the first PIL group were kept individually in perforated plastic boxes containing moistened cotton. Since *P. fuscipes* larvae take up PPE via feeding on eggshells harboring PPE, the eggs of the second PUL group were soaked in a tetracycline solution (5 mg/mL) 3 times (10 min per time) to eliminate PPE from the shell surface (Song et al. 2024). Then they were soaked in sterile water to remove any remaining tetracycline solution and kept individually in perforated plastic boxes as for PUL. The two lines were reared at 25 °C, 60% relative humidity, a photoperiod of 14 h of light and 10 h of darkness. We used 100 eggs from each line to measure fitness following published protocols (Bong 2012). Once a larva emerged, it was supplied with sterilized mixed feed [ingredients: larvae of flour weevil (*Tenebrio molitor*), pork liver powder and honey = 1:3:1]. At least one larva from each pair set up was used to confirm the infection status. The ketosynthase gene (*PKS*) was amplified for PPE detection according to Piel (Table S1; Piel 2002).

The egg incubation period, development (1st larval instar, 2nd larval instar and pupa), and survival of larvae and adults were recorded daily. Survival rates were calculated according to the Kaplan-Meier method. The corresponding p-value was computed using the log-rank (Mantel-Cox) test. The weight and body length of 2nd larval instars (the 5th day of the stage), pupae (the 5th day) and adults (the 10th day) were measured. After checking for normality and homoscedasticity of the data, we used parametric statistical tests (t-tests) to compare the egg incubation period, development time (1st larval instar, 2nd larval instar and pupa), adult longevity, weight and body length between PIL and PUL, as well as a χ^2 test to examine any departure from a 1:1 adult sex ratio. The analyses were conducted using GraphPad Prism v.7® (GraphPad Software, Inc., La Jolla, USA).

For testing differences in reproduction, beetle pairs were kept in perforated plastic boxes as described by Kellner & Dettner (1995) with some leaves for shelter, and a small dish containing moistened cotton in which to lay eggs. Two types of crosses (PIL male × PUL female and PUL male × PIL

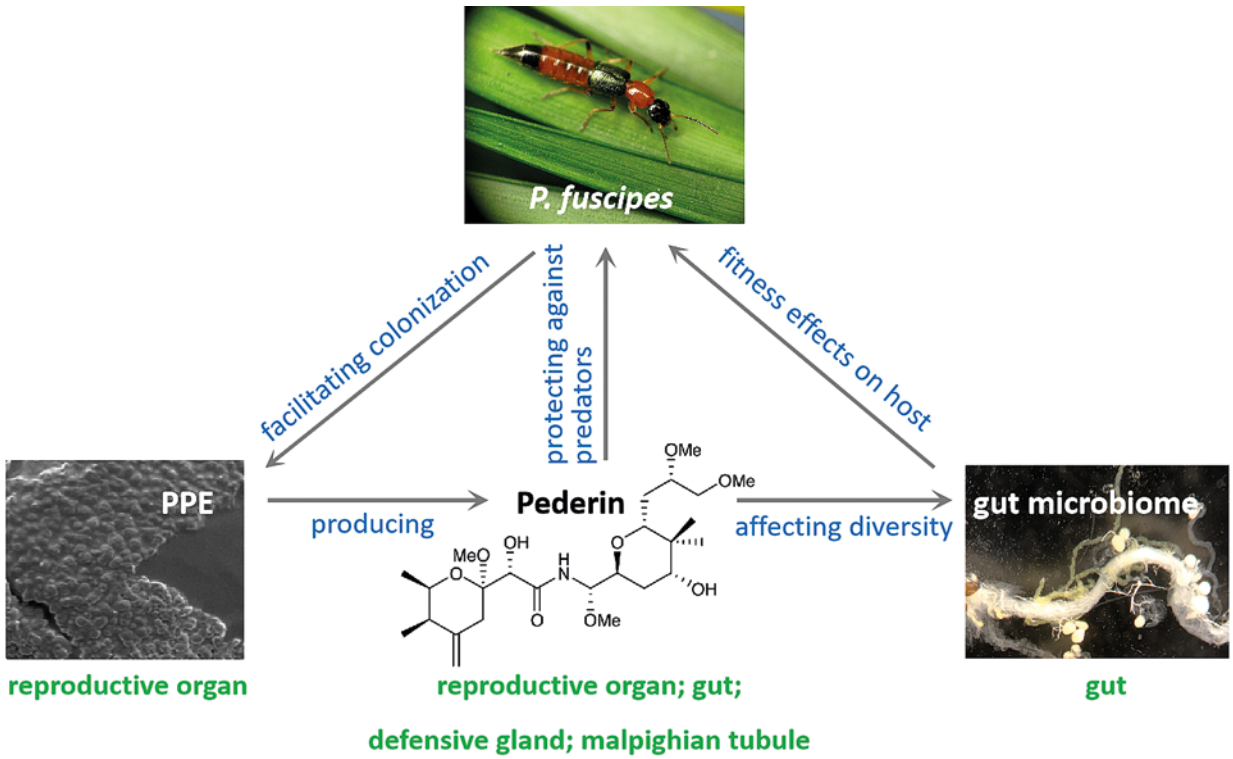

Fig. 1. Potential tripartite interactions among insect, PPE endosymbiont and gut microbiota. PPE produces the toxic substance pederin, which protects the beetles from insect and arachnid predators. The beetle host, in return, provides a favorable environment for the colonization of PPE in female reproductive tissues. Meanwhile, PPE has an effect on the diversity of the gut microbiome by production of pederin and may indirectly alter the fitness of rove beetles. Electron-microscope (SEM) micrographs of a 2-day-old oviposited *Paederus* egg were taken from Kador et al. (2011).

female) were set up in the plastic boxes, with one pair in each box. Crosses within the PIL and PUL lines were also set up. There were 15 replicates for each cross. The small dishes with moistened cotton were checked and eggs were collected and counted every day. The larvae were counted until the last viable egg hatched. Fecundity was expressed as the number of eggs laid in 30 days by the pairs. The hatch rate was expressed as the proportion of hatched eggs over the total number of eggs. We compared fecundity and hatch rate among the four crosses by ANOVA followed by a multiple comparison test (Tukey's posthoc test). All dead individuals expected to be infected were saved and scored again to confirm PPE status after the experiments were finished.

2.2 Microbiota diversity and PPE density in reproductive organs and gusts of *P. fuscipes*

The rove beetles from PIL (3 females and 3 males) and PUL (3 females and 3 males) were dissected. The intestine (including foregut, midgut, and hindgut) and genitalia (including gonads and glands) were cut up and frozen in 70% ethanol at −20 °C. DNA was extracted from 24 specimens respectively with a QIAamp DNA Mini kit (Qiagen, Hilden, Germany) and used for microbiome analysis (Jiang et al. 2018). A 450-bp portion of the 16S rRNA gene was amplifed using the primers (357F and 806R; Table S1) covering the V3–V4 hypervariable regions of bacteria. The library was purified using a DNA gel extraction kit (Axygen, USA) and sequenced by 2*250 bp paired-end sequencing on the Novaseq platform using Novaseq 6000 SP 500 Cycle Reagent Kit (Illumina, USA) at TinyGen Bio-Tech Co., Ltd. Sequences were pre-processed, quality filtered and clustered into operational taxonomic units (OTU) at the 97% sequence similarity level using UPARSE (Edgar 2013). They were annotated and classified utilizing the Silva 138 database with confidence scores ≥ 0.6. The principal component analysis (PCA) of OTU (97% similarity) was done based on relative abundance with prcomp() by built-in R stats package.

The diversity indices (Shannon, Simpson, Chao and ACE) were calculated and plotted by vegan package in R. Significant shifts in the indices were identified using t-tests (Shannon et al. 1950; Cameron et al. 2021). Linear discriminant analysis effect size (LefSe) was used to determine the magnitude of the effect of species abundance on variation in female gut microbiota associated with PIL and PUL, thereby identifying biomarkers that differed significantly in abun-

dance between the two groups. An LDA (linear discriminant analysis) score of > 3 was considered significantly different. PICRUSt was used to investigate the functional profiles of the predictive female gut microbiota associated with PIL and PUL (Langille et al. 2013). The line comparison involved Welch's t-tests with Bonferroni correction to assess differences in the relative abundance of KEGG pathways (level 3) using Statistical Analysis of Metagenomic Profiles (STAMP) (Parks et al. 2014).

To reinforce and confirm metabarcoding data, the relative PPE densities were detected by quantitative PCR (qPCR). It was performed in triplicate for each sample using Platinum SYBR Green (Thermo Fisher Scientific, California, USA) referring to the manufacturer's protocol. The reactions were performed in a total volume of 20 µl comprising 10 µl of 2X Platinum SYBR Green, 0.4 µl (5 µM) of each primer and 1 µl (final 5 ng) template DNA. Following Ali et al. (2018), the relative PPE density was calculated as the ratio of Cq values between *PKS* and the host's endogenous control gene ribosomal protein S3 (*RPS3*), which is synonymous to the number of PPE per host cells because both genes occur as a single copy per haploid genome. The short fragment length (157 bp) of PPE targeted primer pair (KS1-F and KS1-R; Table S1) was used and normalized with a 191bp fragment length of the reference gene (RPS3-F and RPS3-R; Table S1) (Piel 2002; Zhang et al. 2017). The temperature profile of the qPCR was 96 °C for 5 minutes, 35 cycles of 96 °C for 30 s, 57 °C for 30 s, and 72 °C for 1 min with fluorescence acquisition of 72 °C at the end of each cycle, then a melting curve analysis after the final cycle. Assays were conducted as three technical replicates. We checked for normality and homoscedasticity of the data prior to using parametric statistical tests. We compared PPE infection densities in reproductive organ and gut of *P. fuscipes* with a different gender and PPE infection status by ANOVA followed by a multiple comparison test (Tukey's posthoc test) using GraphPad Prism v.7® (GraphPad Software, Inc., La Jolla, USA).

2.3 PPE genome sequencing and gene contents

Pseudomonas sp. Pf01 was isolated from the reproductive tissue of a female *P. fuscipes* from Nanyang, China. The ovaries were dissected, homogenized and streaked out on Columbia agar (Oxoid, UK) supplemented with 5% sheep blood (Solarbio, China). Colonies were screened using *exotoxin A* (*ETA*) and *PKS* genes sequencing (Table S1; Piel 2002; Gray et al. 1984), where the strain was identified as closely related to *Pseudomonas* species. For PacBio sequencing, high molecular weight DNA was extracted from EasyPure Bacteria Genomic DNA Kit (TransGen Biotech, China) following the 15–20 kb SMRTbell Libraries Protocol. The libraries were sequenced using the P6-C4 chemistry on a PacBio Sequel II sequencing platform (PacBio) at Shanghai OE Biotech Co., Ltd (Shanghai, China). For genome resequencing, the NGS libraries were constructed with TruSeq Nano DNA LT Sample Preparation Kit (Illumina, San Diego, CA, USA) and sequenced on the Illumina HiSeq X Ten technology platform (Illumina Inc., San Diego, CA, USA) and 150 bp paired-end reads were generated.

Hierarchical Indexing for Spliced Alignment of Transcripts (HISAT) v2.10.2 (Kim et al. 2015) was used to check the quality of the raw reads and to align to the genome. The filtered clean reads were subjected to de novo genome assembly using Wtdbg2 (Ruan & Li 2020), which is a third-generation assembly technology. The PF01 genome was assembled using K-mer Analysis Toolkit (KAT) v2.4.1 with parameters "-m 27" to estimate the K-mer (Marçais & Kingsford 2011) distribution. GenomeScope was used to calculate estimates for genome size and heterozygosity. N50 size, contig number, and genome size were just a few of the metrics considered in choosing the best genome assembly for downstream analysis. The PF01 genome was annotated with Rapid Annotation using Subsystem Technology (RAST) (Aziz et al. 2008). The genomic synteny involved in pederin family compound biosynthesis genes including symbiont bacterium *Profftella armatura* of Asian citrus psyllid *Diaphorina citri* diaphorin biosynthesis gene (Genbank accession number CP003468), symbiont bacterium PPE of *P. fuscipes* pederin biosynthesis gene (Genbank accession number AY426537, AH013687), symbiont bacterium *Entotheonella* sp. of *Theonella swinhoei* onnamide biosynthesis gene (Genbank accession number AY688304), symbiont bacterium *Nostoc* sp. of *Peltigera membranacea cyanobiont* nosperin biosynthesis gene cluster (Genbank accession number GQ979609) and free-living cyanobacterium *Cuspidothrix issatschenkoi* cusperin gene cluster (Genbank accession number MG518226). They were tandemly compared using Easyfig and the BLASTn algorithm (Sullivan et al. 2011). BLAST comparisons (BLASTn) between multiple genomic regions can be generated, visualized and interactively coloured by Easyfig.

2.3.1 Data availability statement

The 16S rRNA sequences determined in this study were deposited in the Bioproject of The National Center for Biotechnology Information (NCBI) under accession number PRJNA1037296 (https://www.ncbi.nlm.nih.gov/bioproject/PRJNA1037296). The raw genomic data for genome annotation reported in this paper have been deposited in the NCBI database under accession number PRJNA1037318 (https://www.ncbi.nlm.nih.gov/bioproject/PRJNA1037318).

3 Results

3.1 Fitness assessments

In this study, more than 95% of the eggs hatched. The development time of every individual and age-stage survival rate were recorded daily (Table S2; S3), as illustrated by the overlapping curves shown in Fig. 2a. Except for the 1st larval instar stage, the development time of the other immature

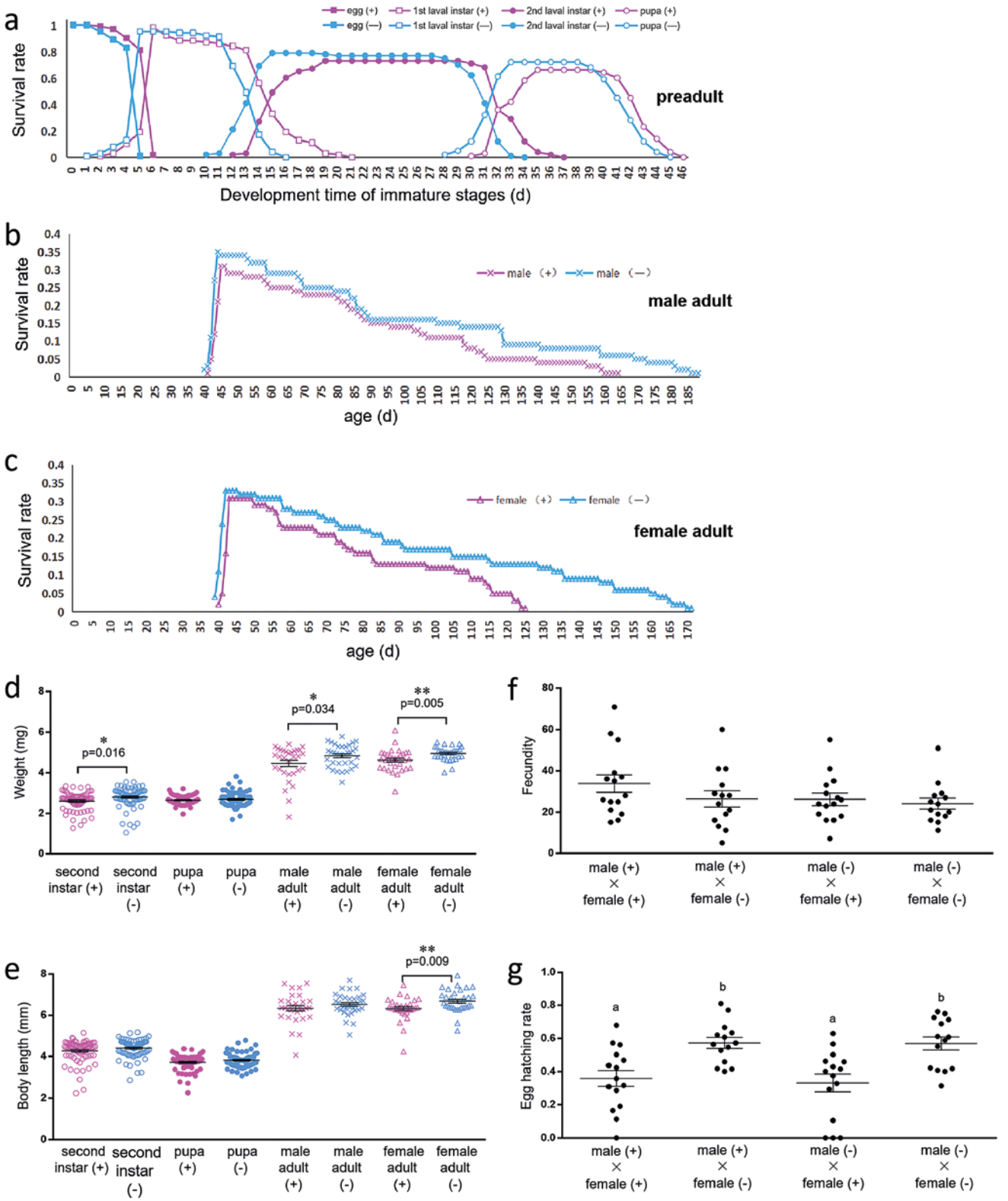

Fig. 2. Survival rate of *P. fuscipes* from PPE-infected and PPE-uninfected lines at different development stage including (a) preadult, (b) male adult, and (c) female adult stages. Dot plots for (d) weight and (e) body length of PIL and PUL at different development stages; (f) fecundity and (g) egg hatching rate of the four crosses. Please find the number of individuals in each line and statistical test in Table 1.

stages (egg, 2nd larval instar and pupa) as well as that of the total immature stage differed significantly between PIL and PUL (Table 1). The adult sex ratios of PIL (31 females and 31 males) and PUL (32 females and 35 males, $\chi^2 = 0.004$, $p = 0.950$) did not vary from 1:1 expectation. After the adults emerged, survival rate of both lines leveled off for 45 d and then decreased gradually (Fig. 2b and 2c). PPE infection had no significant effect on the male adult's life span ($p = 0.055$) by a Log-rank Mantel-Cox test but greatly reduced the female adult's life span ($p = 0.008$). The weight of PIL 2nd larval instars, male adults and female adults was significantly less than those from the PUL line (Fig. 2d). There was no impact of the infection on pupal weight (Table 1; S4). The body length of PIL female adults was significantly shorter than those from the PUL line (Fig. 2e; Table 1; S5). The PPE infection decreased weight and constrained body length of PIL female adults. Fecundity did not differ significantly among the four crosses ($F_{(3,54)} = 1.463$, $p = 0.235$; Fig. 2f; Table S6). However, the egg hatching rates varied among the four crosses ($F_{(3,54)} = 8.303$, $p = 0.0001$; Table S7). The hatching rates of the crosses PUL male × PIL female and PIL male × PIL female were lower than those of the other two crosses (Fig. 2g).

3.2 PPE are shaping the gut microbiome of *P. fuscipes*

Raw sequences of 16S rRNA were used to characterize community diversity and these clustered into 606 operational taxonomic units (OTUs) across the 24 samples tested. Sufficient sequencing data were obtained based on the plateaued rarefaction curves of clearly defined species (Fig. S1). Based on the OTU abundance information (97% similarity), the relative abundance of each OTU in each sample was calculated, and PCA of OTU was done based on relative abundance (Fig. S2). PCA analysis showed variation in community composition in eight groups. The OTUs were annotated into 19 phyla, 33 classes, 70 orders, 115 families and 203 genera (Table S8), of which 14 OTUs were shared among the eight groups (Fig. S3) and 5 OTUs were shared across all samples (Fig. S4). They were *Apibacter adventoris* (relative abundance, 29.54%), *Sphingobacterium* (20.54%), *Bartonella* (11.67%), *Wolbachia* (11.17%) and *Dysgonomonas* (3.24%). When adding the dominant bacterial PPE in female reproductive organs (15.38%), these six phylotypes accounted for 91.54% of the sequences from all samples. The relative abundance of every remaining bacterium was less than 1%, which showed an uneven structure of the bacterial communities in *P. fuscipes* samples.

Table 1. Development time of immature stages, adult longevity, weight and body length of PIL and PUL. L1, 1st larval instar; L2, 2nd larval instar.

Initial eggs in both lines = 100	PIL		PUL		Statistical Results
	n	Mean ± SE	n	Mean ± SE	
Dev. time (d)					
Egg	98	5.66 ± 0.78	95	4.74 ± 0.74	$X^2 = 99.27$; df = 1; $p < 0.001$ ***
L1	98	9.69 ± 2.49	95	9.63 ± 1.03	$X^2 = 4.913$; df = 1; $p = 0.057$
L2	73	20.67 ± 1.28	77	18.47 ± 1.19	$X^2 = 84.63$; df = 1; $p < 0.001$ ***
Pupa	66	10.41 ± 1.94	72	11.90 ± 1.80	$X^2 = 16.05$; df = 1; $p < 0.001$ ***
Total immature	62	44.98 ± 3.67	68	43.81 ± 2.46	$X^2 = 3.675$; df = 1; $p < 0.001$ ***
Adult longevity (d)					
Male	31	53.97 ± 33.92	35	68.74 ± 43.68	$X^2 = 3.675$; df = 1; $p = 0.055$
Female	31	45.87 ± 26.16	33	65.13 ± 39.54	$X^2 = 6.878$; df = 1; $p = 0.008$ **
Weight (mg)					
L2	73	2.61 ± 0.43	77	2.78 ± 0.48	$t = 2.447$; df = 148; $p = 0.016$ *
Pupa	66	2.64 ± 0.23	72	2.68 ± 0.35	$t = 0.820$; df = 136; $p = 0.414$
Male	31	4.46 ± 0.85	35	4.84 ± 0.54	$t = 2.165$; df = 64; $p = 0.034$ *
Female	31	4.63 ± 0.53	33	4.96 ± 0.33	$t = 2.943$; df = 62; $p = 0.005$ **
Body length (mm)					
L2	73	4.26 ± 0.53	77	4.40 ± 0.44	$t = 1.662$; df = 148; $p = 0.099$
Pupa	66	3.72 ± 0.38	72	3.82 ± 0.34	$t = 1.665$; df = 135; $p = 0.098$
Male	31	6.32 ± 0.71	35	6.52 ± 0.51	$t = 1.253$; df = 64; $p = 0.215$
Female	31	6.31 ± 0.55	33	6.68 ± 0.53	$t = 2.700$; df = 62; $p = 0.009$ *

Bacterial species diversity showed a significant difference among the eight groups (Fig. S5). The relative abundance of specific groups also varied (Table S9). The 16S rRNA gene data revealed microbial community structure across groups at the genus level (Fig. 3). Notably, the five core bacteria showed effects of PPE. The relative abundance of PPE in reproductive organs was positively associated to *Bartonella* in the guts, but was inversely related to *Apibacter* in guts, as well as *Wolbachia* and *Sphingobacterium* in reproductive organs (Fig. 3). In the LefSe analysis, Flavobacteriaceae at the class level, Flavobacteriales at the order level were abundant in the female gut of PUL. *Apibacter* was elevated, and *Bartonella* and *Lactobacillus* were reduced at the genus level in the female gut of PUL (LDA score > 3, P < 0.05) (Fig. S6). Among the 157 affiliated KEGG pathways, 35 were significantly different at P < 0.001 (Fig. S7, Table S10). Notably, significant elevation in ABC transporters, polyketide products biosynthesis and metabolism of xenobiotics by cytochrome P450 pathways was observed in PIL. On the other hand, pathways related to host fitness advantages (e.g. metabolism, longevity regulating pathway, MAPK signaling pathway and vancomycin resistance) was increased in PUL.

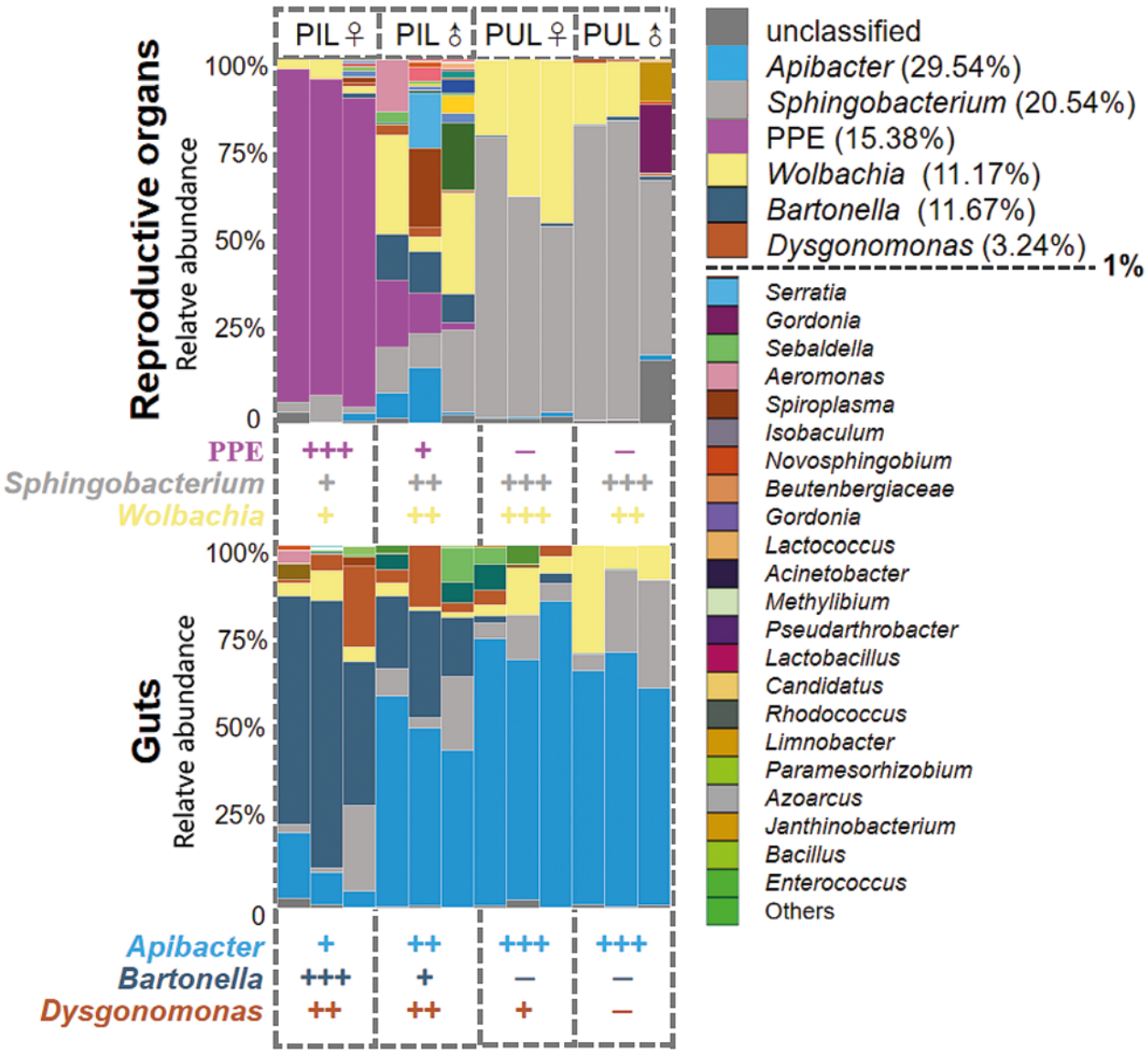

Fig. 3. Bacterial 16S rRNA gene composition in terms of gender (males and females), organs (guts and reproductive organs) of *P. fuscipes*. Eight groups were separated with dashed lines (PIL, PPE-infected line; PUL, PPE-uninfected line). Each group consisted of 3 replicates. The relative abundance of only five annotated genera were over 1%. PPE and *Wolbachia* were the core bacteria in reproductive organs, and *Apibacter, Sphingobacterium, Bartonella* and *Dysgonomonas* were the core bacteria in guts. +++, high content (> 50%); ++, medium content (20–50%); +, low content (0–20%); –, n/a.

The PPE density analyzed through qPCR targeting the specific *PKS* gene along with an endogenous control gene *RPS3* varied significantly ($F_{(7,64)}$=50.26, $p < 0.0001$) across the reproductive organs and guts of *P. fuscipes* with a different gender. The infection density in reproductive organs of PIL females was significantly higher than in any other group and some PPE were examined in reproductive organs of PIL males (Fig. S8). The results correspond well with metabarcoding data of 16S rRNA.

3.3 PPE genome sequencing and gene contents

Whole-genome sequencing using PacBio and Illumina technologies led to the assembly of a circular 6.66 Mb *Pseudomonas* sp. Pf01 symbiont genome, containing 6109 coding sequences (CDS), 66.3% GC content and with a BUSCO completeness score of 89.44% (Fig. S9; Table S11). The genome showed full completeness and was similar to *Pseudomonas aeruginosa* (6.26 Mb, Genbank accession number: GCA_000006765.1). We compared pederin family biosynthetic gene clusters from symbiotic organisms of diverse evolutionary origin (Fig. S10). This confirmed the genome of PPE contains the unique *ped* genes encoding megaenzymes PKSs/NRPSs, which catalyze the synthesis of the polyketone compound pederin. The *ped* gene cluster consists of a 54-kb region with 3 large genes (pedI, pedF, and pedH) that encode multidomain PKS or PKS/NRPS proteins and a suite of 14 smaller genes that encode accessory enzymes (Fig. S10). It has significant homology to the gene clusters for the biosynthesis of pederin family compounds diaphorin isolated from the Asian citrus psyllid *Diaphorina citri*, onnamide A from sponge *Theonella swinhoei*, nosperin isolated from the foliose lichen *Peltigera membranacea* and cusperin isolated from the free-living cyanobacterium *Cuspidothrix issatschenkoi* (Kampa et al. 2013; Kust et al. 2018; Nakabachi et al. 2013; Piel et al. 2004; Kim et al. 2020).

4 Discussion

PPE are concentrated in female reproductive tissues of the rove beetle and harbored on the egg shells based on FISH (Fang et al. 2023; Kador et al. 2011). The *Paederus* larvae take up PPE via feeding on eggshell, forming a way of egg shell-oral transmission (Kellner 2003). However, the insect gut bacteria were acquired from environmental habitat and diet, and also determined by developmental stage and phylogeny of host (Yun et al. 2014). Thus, we soaked the eggs in a tetracycline solution to eliminate PPE from the shell surface as for endosymbiont-free group in this study, which minimizes the effects of antibiotic treatment on the microbiota associated with the gut and reproductive system. The similar method was reported in a recently published paper (Song et al. 2024).

The current work highlighted strong deleterious fitness effects of the PPE infection on *P. fuscipes*. The fitness costs relate to an extended development time, shortened lifespan of female adults, light weight and short body length especially for infected female adults (Fig. 2a–2e and Table 1), as well as a significantly lower hatch rates of crosses with PIL females (Fig. 2g). These notable deleterious fitness effects run counter to previous perspectives of mutualistic symbiosis between *P. fuscipes* and PPE (Fang et al. 2023). However, there are many other symbioses that involve costs as well as benefits to one of the parties (Li et al. 2022; Bronstein 2001). Cost/benefit analysis has long been a standard approach in studying the ecological dynamics of such interactions (Keeler 1985). The ecology and evolution of mutualism is shaped by diverse costs and benefits that they confer (Bronstein 2001). Costs or constraints always need to be included in understanding the population dynamics of mutualists and their stable co-existence (Nakabachi et al. 2013).

While acidic pederin produced from PPE is corrosive, it may not directly contribute to the fitness disadvantages of *P. fuscipes* because most pederin occurs in the defensive gland with reservoirs inside *P. fuscipes* as chemical weapons against potential predators (Stromgaard et al. 2001; Kellner 2002). Instead, we suspect that the remaining pederin absorbed by malpighian tubules from hemolymph may have influenced the composition and relative abundance of gut bacteria when it was discharged through the transition of the midgut and rectum (Fig. S11; Bhandari et al. 2015). The fitness costs caused by PPE infection may be linked to the change of community structure of the gut microbiome which can influence life history traits associated with host fitness such as development, longevity and fecundity in organisms (Di Lelio et al. 2023; Gao et al. 2023). Thus, 16S rRNA gene sequencing was used to compare the community diversity and abundance between PIL and PUL, and to reveal the potential pattern of PPE-microbe interactions.

Based on the results of 16S rRNA gene sequencing, *Apibacter* (29.5%), PPE (15.4%), *Bartonella* (11.7%), *Wolbachia* (11.2%) and *Dysgonomonas* (3.2%) were five identified genera accounting for the largest proportions (3–30%) of microorganisms in adult *P. fuscipes*. These core bacteria were reported in the previous studies (Fang et al. 2023; Teoh & Singham 2022). While PPE did not show an association with *Dysgonomonas*, it strongly affected the other three microbial taxa. *Apibacter* was recently identified as a genus of bee associated bacteria, which is putatively beneficial to the host including decreasing a trypanosome parasite infection and degrading toxic monosaccharides and dicarboxylic acids (Mockler et al. 2018; Zhang et al. 2022). *Bartonella* sp. is an etiological agent of bartonellosis (Breitschwerdt et al. 2010). This arthropod-borne pathogen was found in the hematophageous fleas, and contributed to a fitness reduction to the hosts; infected female fleas had smaller male progeny (Morick et al. 2013). PPE infection

resulted in a decrease in the number of beneficial symbiotic bacteria *Apibacter* and an increase in the number of conditional pathogenic bacteria *Bartonella*. Although the symbiotic relationships between the two bacteria and *P. fuscipes* are so far unexplored, their relative abundance seems to link to fitness of their host as in the other insects mentioned above. The abundance of *Apibacter* and *Bartonella* were likely affected by pederin and PPE.

Another core bacterium negatively associated with PPE is *Wolbachia* in reproductive tissues. *Wolbachia* (Hoffmann 2020) mainly live inside cells of arthropods, especially in insects and some nematodes, and can affect sexual reproduction of their hosts. One of the most important phenotypes induced by *Wolbachia* is cytoplasmic incompatibility (CI), where *Wolbachia* uninfected females mated to infected males show a sharp reduction in production of viable offspring. This may relate to our results on egg hatching rates varying significantly among the four crosses (Table 1). The decrease in abundance of *Wolbachia* in PIL (Fig. 3) may contribute to a significantly lower hatching rate in crosses PUL male × PIL female and PIL male × PIL female (Fig. 2g).

We propose a microbe-microbe interaction pattern involving the metabolites pederin travelling in the digestive system to influence other microbes, and thereby indirectly influence host-microbe interactions influencing the fitness, immunity and metabolism of *P. fuscipes*. Despite this, over 90% of female beetles carry PPE and transfer it to their progeny in nature linked to advantages for their survival under predation (Kellner 2002), although there is then also phenomenon of automimicry (analogous to Batesian mimicry within a single prey species) for non-defended individuals (Teoh & Singham 2022). Compared with the situation in a natural population, the number of infected females in lab-reared generations was reduced over time likely due to the absence of predation risk (Kellner 2000). This suggests there is likely a trade-off between fitness and protection against predation in *P. fuscipes*. Overall, our findings emphasize the importance of tripartite interactions among microbiota, *P. fuscipes*, and PPE from a holobiont perspective (Zheng et al. 2023) and raise intriguing ecological and evolutionary questions.

Acknowledgments: We thank Zhong Peng and their colleagues (Shanghai Normal University, Shanghai, China) for providing valuable comments and specimens throughout the project. We thank the technical support from OEbiotech Inc. and TinyGene Bio-Tech. This study was financially supported by grants from Natural Science Foundation of Shanghai (20ZR1440800), Shanghai Municipal Human Resources and Social Security Bureau (2019112) and Shanghai Normal University (SK202143).

References

Antwis, R. E., Griffiths, S. M., Harrison, X. A., Aranega-Bou, P., Arce, A., Bettridge, A. S., … Sutherland, W. J. (2017). Fifty important research questions in microbial ecology. *FEMS Microbiology Ecology, 93*(5), fix044. https://doi.org/10.1093/femsec/fix044

Ali, H., Muhammad, A., Islam, S. U., Islam, W., & Hou, Y. M. (2018). A novel bacterial symbiont association in the hispid beetle, *Octodonta nipae* (Coleoptera: Chrysomelidae), their dynamics and phylogeny. *Microbial Pathogenesis, 118*, 378–386. https://doi.org/10.1016/j.micpath.2018.03.046

Aziz, R. K., Bartels, D., Best, A. A., DeJongh, M., Disz, T., Edwards, R. A., … Zagnitko, O. (2008). The RAST Server: Rapid annotations using subsystems technology. *BMC Genomics, 9*(1), 75. https://doi.org/10.1186/1471-2164-9-75

Bhandari, D. R., Schott, M., Römpp, A., Vilcinskas, A., & Spengler, B. (2015). Metabolite localization by atmospheric pressure high-resolution scanning microprobe matrix-assisted laser desorption/ionization mass spectrometry imaging in whole-body sections and individual organs of the rove beetle Paederus riparius. *Analytical and Bioanalytical Chemistry, 407*(8), 2189–2201. https://doi.org/10.1007/s00216-014-8327-1

Bong, L. J., Neoh, K. B., Jaal, Z., & Lee, C. Y. (2012). Life Table of *Paederus fuscipes* (Coleoptera: Staphylinidae). *Journal of Medical Entomology, 49*(3), 451–460. https://doi.org/10.1603/ME11163

Breitschwerdt, E. B., Maggi, R. G., Chomel, B. B., & Lappin, M. R. (2010). Bartonellosis: An emerging infectious disease of zoonotic importance to animals and human beings. *Journal of Veterinary Emergency and Critical Care (San Antonio, Tex.), 20*(1), 8–30. https://doi.org/10.1111/j.1476-4431.2009.00496.x

Bronstein, J. L. (2001). The costs of mutualism. *American Zoologist, 41*(4), 825–839.

Cameron, E. S., Schmidt, P. J., Tremblay, B. J., Emelko, M. B., & Müller, K. M. (2021). Enhancing diversity analysis by repeatedly rarefying next generation sequencing data describing microbial communities. *Scientific Reports, 11*(1), 22302. https://doi.org/10.1038/s41598-021-01636-1

Di Lelio, I., Forni, G., Magoga, G., Brunetti, M., Bruno, D., Becchimanzi, A., … Pennacchio, F. (2023). Soil fungus confers plant resistance against a phytophagous insect by disrupting the symbiotic role of its gut microbiota. *Proceedings of the National Academy of Sciences of the United States of America, 120*(10), e2216922120. https://doi.org/10.1073/pnas.2216922120

Douglas, A. E. (1998). Nutritional interactions in insect-microbial symbioses: Aphids and their symbiotic bacteria *Buchnera*. *Annual Review of Entomology, 43*(1), 17–37. https://doi.org/10.1146/annurev.ento.43.1.17

Edgar, R. C. (2013). UPARSE: Highly accurate OTU sequences from microbial amplicon reads. *Nature Methods, 10*(10), 996–998. https://doi.org/10.1038/nmeth.2604

Fang, J., Wang, Y. Q., Hu, J. Y., Hoffmann, A. A., Li, L. Z., Yin, Z. W., … Jiang, W. B. (2023). Dissecting a mutualistic interaction involving an insect-endosymbiont association. *Entomologia Generalis, 43*(2), 399–407. https://doi.org/10.1127/entomologia/2022/1697

Gao, H. H., Zhao, S., Wang, R. J., Qin, D. Y., Chen, P., Zhang, A. S., … Zhou, X. H. (2023). Gut bacterium promotes host fitness in special ecological niche by affecting sugar metabolism

in *Drosophila suzukii. Insect Science, 30*(6), 1713–1733. https://doi.org/10.1111/1744-7917.13189

Geller, A. M., & Levy, A. (2023). "What I cannot create, I do not understand": Elucidating microbe-microbe interactions to facilitate plant microbiome engineering. *Current Opinion in Microbiology, 72*, 102283. https://doi.org/10.1016/j.mib.2023.102283

Gray, G. L., Smith, D. H., Baldridge, J. S., Harkins, R. N., Vasil, M. L., Chen, E. Y., & Heyneker, H. L. (1984). Cloning, nucleotide sequence, and expression in *Escherichia coli* of the exotoxin A structural gene of *Pseudomonas aeruginosa. Proceedings of the National Academy of Sciences of the United States of America, 81*(9), 2645–2649. https://doi.org/10.1073/pnas.81.9.2645

Hoffmann, A. A. (2020). Wolbachia. *Current Biology, 30*(19), R1113–R1114. https://doi.org/10.1016/j.cub.2020.08.039

Jiang, W. B., Zhu, J. Q., Wu, Y. J., Li, L. Z., Li, Y. Y., Ge, C., … Yu, W. D. (2018). Influence of *Wolbachia* infection on mitochondrial DNA variation in the genus *Polytremis* (Lepidoptera: Hesperiidae). *Molecular Phylogenetics and Evolution, 129*, 158–170. https://doi.org/10.1016/j.ympev.2018.08.001

Kador, M., Horn, M. A., & Dettner, K. (2011). Novel oligonucleotide probes for in situ detection of pederin-producing endosymbionts of *Paederus riparius* rove beetles (Coleoptera: Staphylinidae). *FEMS Microbiology Letters, 319*(1), 73–81. https://doi.org/10.1111/j.1574-6968.2011.02270.x

Kampa, A., Gagunashvili, A. N., Gulder, T. A. M., Morinaka, B. I., Daolio, C., Godejohann, M., … Andrésson, Ó. (2013). Metagenomic natural product discovery in lichen provides evidence for a family of biosynthetic pathways in diverse symbioses. *Proceedings of the National Academy of Sciences of the United States of America, 110*(33), E3129–E3137. https://doi.org/10.1073/pnas.1305867110

Keeler, K. H. (1985). Cost: benefit models of mutualism. In D. Boucher (Ed.), *The biology of mutualism*. Oxford, UK: Oxford University Press.

Kellner, R. L. L. (2000). Possible genetic basis of pederin polymorphism in rove beetles (*Paederus riparius*). *The Journal of Heredity, 91*(2), 158–162. https://doi.org/10.1093/jhered/91.2.158

Kellner, R. L. L. (2001). Suppression of pederin biosynthesis through antibiotic elimination of endosymbionts in *Paederus sabaeus. Journal of Insect Physiology, 47*(4–5), 475–483. https://doi.org/10.1016/S0022-1910(00)00140-2

Kellner, R. L. L. (2002). Molecular identification of an endosymbiotic bacterium associated with pederin biosynthesis in *Paederus sabaeus* (Coleoptera: Staphylinidae). *Insect Biochemistry and Molecular Biology, 32*(4), 389–395. https://doi.org/10.1016/S0965-1748(01)00115-1

Kellner, R. L. L. (2003). Stadium-specific transmission of endosymbionts needed for pederin biosynthesis in three species of *Paederus* rove beetles. *Entomologia Experimentalis et Applicata, 107*(2), 115–124. https://doi.org/10.1046/j.1570-7458.2003.00042.x

Kellner, R. L. L., & Dettner, K. (1995). Allocation of pederin during lifetime of *paederus* rove beetles (Coleoptera: staphylinidae): evidence for polymorphism of hemolymph toxin. *Journal of Chemical Ecology, 21*(11), 1719–1733. https://doi.org/10.1007/BF02033672

Kim, D., Langmead, B., & Salzberg, S. L. (2015). HISAT: A fast spliced aligner with low memory requirements. *Nature Methods, 12*(4), 357–360. https://doi.org/10.1038/nmeth.3317

Kim, Y. J., Park, H. K., & Kim, I. S. (2020). Invasion and toxin production by exotic nostocalean cyanobacteria (*Cuspidothrix, Cylindrospermopsis*, and *Sphaerospermopsis*) in the Nakdong River, Korea. *Harmful Algae, 100*, 101954. https://doi.org/10.1016/j.hal.2020.101954

Kust, A., Mareš, J., Jokela, J., Urajová, P., Hájek, J., Saurav, K., … Hrouzek, P. (2018). Discovery of a Pederin family compound in a nononsymbiotic bloom-forming Cyanobacterium. *ACS Chemical Biology, 13*(5), 1123–1129. https://doi.org/10.1021/acschembio.7b01048

Langille, M. G. I., Zaneveld, J., Caporaso, J. G., McDonald, D., Knights, D., Reyes, J. A., & Huttenhower, C. (2013). Predictive functional profiling of microbial communities using 16S rRNA marker gene sequences. *Nature Biotechnology, 31*(9), 814–821. https://doi.org/10.1038/nbt.2676

Li, T. P., Zhou, C. Y., Wang, M. K., Zha, S. S., Chen, J., Bing, X. L., … Hong, X. (2022). Endosymbionts reduce microbiome diversity and modify host metabolism and fecundity in the Planthopper *Sogatella furcifera. mSystems, 7*(2), 01516–01521. https://doi.org/10.1128/msystems.01516-21

Marçais, G., & Kingsford, C. (2011). A fast, lock-free approach for efficient parallel counting of occurrences of k-mers. *Bioinformatics (Oxford, England), 27*(6), 764–770. https://doi.org/10.1093/bioinformatics/btr011

McCutcheon, J. P., Boyd, B. M., & Dale, C. (2019). The life of an insect endosymbiont from the cradle to the grave. *Current Biology, 29*(11), R485–R495. https://doi.org/10.1016/j.cub.2019.03.032

Mockler, B. K., Kwong, W. K., Moran, N. A., & Koch, H. (2018). Microbiome structure influences infection by the parasite *Crithidia bombi* in bumble bees. *Applied and Environmental Microbiology, 84*(7), e02335–e17. https://doi.org/10.1128/AEM.02335-17

Morick, D., Krasnov, B. R., Khokhlova, I. S., Gutiérrez, R., Fielden, L. J., Gottlieb, Y., & Harrus, S. (2013). Effects of *Bartonella* spp. on Flea Feeding and Reproductive Performance. *Applied and Environmental Microbiology, 79*(11), 3438–3443. https://doi.org/10.1128/AEM.00442-13

Nakabachi, A., Ueoka, R., Oshima, K., Teta, R., Mangoni, A., Gurgui, M., … Fukatsu, T. (2013). Defensive bacteriome symbiont with a drastically reduced genome. *Current Biology, 23*(15), 1478–1484. https://doi.org/10.1016/j.cub.2013.06.027

Parks, D. H., Tyson, G. W., Hugenholtz, P., & Beiko, R. G. (2014). STAMP: Statistical analysis of taxonomic and functional profiles. *Bioinformatics (Oxford, England), 30*(21), 3123–3124. https://doi.org/10.1093/bioinformatics/btu494

Piel, J. (2002). A polyketide synthase-peptide synthetase gene cluster from an uncultured bacterial symbiont of *Paederus* beetles. *Proceedings of the National Academy of Sciences of the United States of America, 99*(22), 14002–14007. https://doi.org/10.1073/pnas.222481399

Piel, J., Hui, D., Wen, G., Butzke, D., Platzer, M., Fusetani, N., & Matsunaga, S. (2004). Antitumor polyketide biosynthesis by an uncultivated bacterial symbiont of the marine sponge *Theonella swinhoei. Proceedings of the National Academy of Sciences of the United States of America, 101*(46), 16222–16227. https://doi.org/10.1073/pnas.0405976101

Ruan, J., & Li, H. (2020). Fast and accurate long-read assembly with wtdbg2. *Nature Methods, 17*(2), 155–158. https://doi.org/10.1038/s41592-019-0669-3

Shannon, C. E., Weaver, W., & Wiener, N. (1950). The mathematical theory of communication. *Physics Today, 3*(9), 31–32. https://doi.org/10.1063/1.3067010

Song, X., Huang, T., Yan, X., Zuo, M., Pan, Y., He, H., … Yang, T. (2024). The pederin-producing bacteria density dynamics in *Paederus fuscipes* at different developmental stages. *Medical and Veterinary Entomology, 38*(1), 59–72. https://doi.org/10.1111/mve.12697

Stromgaard, K., Andersen, K., Krogsgaard-Larsen, P., & Jaroszewski, J. W. (2001). Recent advances in the medicinal chemistry of polyamine toxins. *Current Medicinal Chemistry, 1*(4), 317–338.

Sullivan, M. J., Petty, N. K., & Beatson, S. A. (2011). Easyfig: A genome comparison visualizer. *Bioinformatics (Oxford, England), 27*(7), 1009–1010. https://doi.org/10.1093/bioinformatics/btr039

Teoh, M., & Singham, G. V. (2022). Bacterial diversity and community structure shapes pederin polymorphism but lacks association with host genotype specificity in the rove beetle, *Paederus fuscipes. FEMS Microbiology Ecology, 98*(9), 1–12. https://doi.org/10.1093/femsec/fiac087

Willing, B. P., Russell, S. L., & Finlay, B. B. (2011). Shifting the balance: Antibiotic effects on host-microbiota mutualism. *Nature Reviews. Microbiology, 9*(4), 233–243. https://doi.org/10.1038/nrmicro2536

Yun, J., Roh, S., Whon, T., Jung, M., Kim, M., Park, D., … Bae, J. (2014). Insect gut bacterial diversity determined by environmental habitat, diet, developmental stage, and phylogeny of host. *Applied and Environmental Microbiology, 80*(17), 5254–5264. https://doi.org/10.1128/AEM.01226-14

Zhang, H., Tang, B., Lin, Y., Chen, Z., Zhang, X., Ji, T., … Hou, Y. M. (2017). Identification of three prophenoloxidase-activating factors (PPAFs) from an invasive beetle *Octodonta nipae* Maulik (Coleoptera: Chrysomelidae) and their roles in the prophenoloxidase activation. *Archives of Insect Biochemistry and Physiology, 96*(4), e21425. https://doi.org/10.1002/arch.21425

Zhang, W. J., Zhang, X., Su, Q. Z., Tang, M., Zheng, H., & Zhou, X. (2022). Genomic features underlying the evolutionary transitions of *Apibacter* to honey bee gut symbionts. *Insect Science, 29*(1), 259–275. https://doi.org/10.1111/1744-7917.12912

Zheng, R. E., Wang, Q. Q., Wu, R. B., Paradkar, P. N., Hoffmann, A. A., & Wang, G. H. (2023). Holobiont perspectives on tripartite interactions among microbiota, mosquitoes, and pathogens. *The ISME Journal, 17*(8), 1143–1152. https://doi.org/10.1038/s41396-023-01436-7

Zvereva, E. L., & Kozlov, M. V. (2016). The costs and effectiveness of chemical defenses in herbivorous insects: A meta-analysis. *Ecological Monographs, 86*(1), 107–124. https://doi.org/10.1890/15-0911.1

Manuscript received: January 12, 2024
Revisions requested: March 21, 2024
Revised version received: May 29, 2024
Manuscript accepted: July 4, 2024

The pdf version (Adobe JavaScript must be enabled) of this paper includes an electronic supplement. Please download the supplement and rename the file extension to .zip:

Table S1–S11; Figure S1–S11